On the Fundamental Particles and Reactions of Nature

Jian-Bin Bao[1,2*] and Nicholas P. Bao[3,4†]

1. Zhejiang University Alumni Association, Hangzhou, Zhejiang 310027, P. R. China;
2. University of Alberta Alumni Association, Edmonton, Alberta T5J 4P6, Canada;
3. Archbishop MacDonald Catholic High School, Edmonton, Alberta T5N 1H5, Canada;
4. Faculty of Science, University of Alberta, Edmonton, Alberta T6G 2E1, Canada
* E-mail: jbbao@hotmail.com; † E-mail: nbao@ualberta.ca.

Abstract: There are unsolved problems related to inflation, gravity, dark matter, dark energy, missing antimatter, and the birth of the universe. Some of them can be better answered by assuming the existence of aether and hypoatoms. Both were created during the inflation in the very early universe. While aether forms vacuum, hypoatoms, composed of both matter and antimatter and believed to be neutrinos, form all observable matter. In vacuum, aether exists between the particle-antiparticle dark matter form and the dark energy form in a dynamic equilibrium: $A + \overline{A} \rightleftharpoons \gamma + \gamma$. The same reaction stabilizes hypoatoms and generates a 3-dimensional sink flow of aether that causes gravity. Based on the hypoatom structure, the singularity does not exist inside a black hole; the core of the black hole is a hypoatom star or neutrino star. By gaining enough mass, ca. $3 \times 10^{22} M_\odot$, to exceed neutrino degeneracy pressure, the black hole collapses or annihilates into the singularity, thus turning itself into a white hole or a Big Bang. The universe is anisotropic. Its center, or where the Big Bang happened, is at $0.66^{+0.03}_{-0.01}$ times the radius of the observable universe at Galactic coordinates $(l, b) = (286° \pm 10°, -43°^{+7°}_{-6°})$. If we look from the Local Group to the center of the universe, the universe is rotating clockwise.

Keywords: aether; hypoatom; neutrino; inflation; gravity; negative pressure; dark energy; dark matter; black hole; spinning universe; quantum mechanics; first galaxies; spin-1/2 particle; matter-anti-matter asymmetry; baryogenesis-through-leptogenesis; fabric of space; center of the universe; fate of the universe; general theory of relativity

I. INTRODUCTION

For the Schwarzschild metric:

$$ds^2 = -\left(1 - \frac{2GM}{rc^2}\right)c^2 dt^2 + \left(1 - \frac{2GM}{rc^2}\right)^{-1} dr^2 + r^2 d\Omega^2 \tag{1}$$

if we define speed

$$v = \sqrt{2GM/r} \tag{2}$$

we have

$$ds^2 = -\left(1 - \frac{v^2}{c^2}\right)c^2 dt^2 + \left(1 - \frac{v^2}{c^2}\right)^{-1} dr^2 + r^2 d\Omega^2 \tag{3}$$

on the right of which, the first term shows the time dilation effect, and the second term shows the length contraction effect. This unequivocally indicates that the stationary objects in a gravitational field are in motion. The length contraction effect in equation (3) even says that the direction of motion is radial and the speed v of motion is equal to the escape speed $v_{esc} = \sqrt{2GM/r}$. Since motion is always relative to a frame of reference, we can make the stationary objects move by finding the reference frame that is moving in the gravitational field. We therefore believe that there exist fundamental particles. Einstein

once stated[1]: "according to the general theory of relativity, space without aether is unthinkable." We then use the term aether to name the fundamental particles.

II. THEORY

2.1. Creation of fundamental particles

To know what aether could be, we start with the idea of the inflation that was proposed to resolve the horizon, flatness, and magnetic monopole problems[2]. Although the physical mechanism underlying inflation is still uncertain, it is often believed to be the result of a scalar field rolling down from the false vacuum to the true vacuum[3,4]. We study the inflation by proposing the following reactions in the very early universe:

$$E \rightarrow A + \overline{A} \qquad\qquad\qquad \text{(I)}$$
$$i A + i \overline{A} \rightarrow E \ (i \in N, \ i < n) \qquad\qquad \text{(II)}$$
$$n A + n \overline{A} \rightarrow \gamma + \gamma \qquad\qquad \text{(III)}$$
$$\gamma + \gamma \rightarrow B + \overline{B} \qquad\qquad\qquad \text{(IV)}$$
$$B + \overline{B} \rightarrow \gamma + \gamma \qquad\qquad\qquad \text{(V)}$$
$$B + n \overline{A} \rightarrow \gamma + \gamma \qquad\qquad\qquad \text{(VI)}$$
$$\overline{B} + n A \rightarrow \gamma + \gamma \qquad\qquad\qquad \text{(VII)}$$
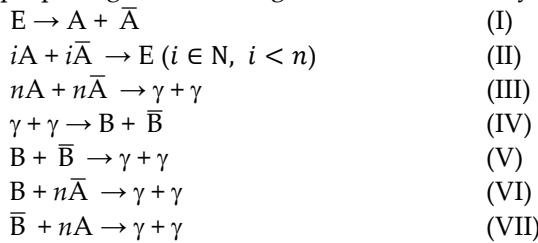
Reaction (I) was the first phase transition in the universe, converting the pure energy (E) of the singularity universe into the particles (A) and antiparticles ($\overline{A}$) that are aether (Fig. 1). This reaction fits in the current inflation theory well. As will be discussed below, the energy of the singularity can be regarded as photons whose wavelength is asymptote to zero. Therefore, the singularity universe was a false vacuum. As its energy was converted into aether particles, the universe became a true vacuum. According to Einstein's mass-energy equivalence principle, matter and antimatter pairs are the only possible products from energy. As Planck taught us that energy is quantized, what the supercooled universe could first create could only be the most fundamental quanta, even though it had sufficient energy to create any complicated particles. The fundamental aether particles A and $\overline{A}$ settled at the lowest mass and in the smallest size with the highest stability possible for them to survive in the hot and dense primeval universe. As the reaction finished, the universe became a globe of aether particles A and $\overline{A}$; the volume of the universe increased exponentially. As the energy of the universe was used up, the temperature of the universe dropped significantly, and the inflation ended naturally.

Right after the creation, aether particles A and $\overline{A}$ were annihilated, raising the temperature of the universe back to what the adiabatic standard cosmology describes (Fig. 1). This is known as the reheating process. In this work, we postulate: *annihilation only happens if an equal amount of matter and antimatter particles are in contact with each other*. Therefore, numerous annihilations initiated simultaneously across the globe of the universe, competing for the remaining aether particles A and $\overline{A}$, and finished together when there were no more A and $\overline{A}$ left in contact. While a pair or a small number ($i < n$) of pairs of A and $\overline{A}$ particles were annihilated to energy (reaction II) due to the wavelengths of products being larger than the size of the universe at that moment, n pairs of aether particles were annihilated to produce photons with a wavelength the size of the universe (reaction III). It is reaction (III) that allowed the universe to deviate from energy and create more complicated particles (discussed below). Of course, the annihilations were impossible to be 100% complete. Some aether particles were left along and therefore survived.

The formed photons then collided to create particles B and antiparticles $\overline{B}$ (Fig.1) by the Breit-Wheeler pair production process (reaction IV). This phase transition has been regarded as the second episode of inflation[5,6], though the universe would not experience a significant change of volume as it was already large. Immediately followed were three possible annihilations to reheat the universe: 1) B and $\overline{B}$ (reaction V); 2) n $\overline{A}$'s with a B (reaction VI, the total amount of matter must be equal to that of antimatter: $n\varepsilon_{\overline{A}} = \varepsilon_B$); and 3) n A's with a $\overline{B}$ (reaction VII, $n\varepsilon_A = \varepsilon_{\overline{B}}$). Because the primeval universe was dense

enough to allow multiple $\overline{A}$'s to contact with a B simultaneously and multiple A's to contact with a $\overline{B}$ simultaneously for annihilation, both reactions (VI) and (VII) were possible, but their reaction rates did not have to be equal.

Although the reaction parameters are difficult to know, these proposed reactions provide a possible mechanism of the inflation and reheating. More importantly, it is the products of these reactions that formed the observable universe.
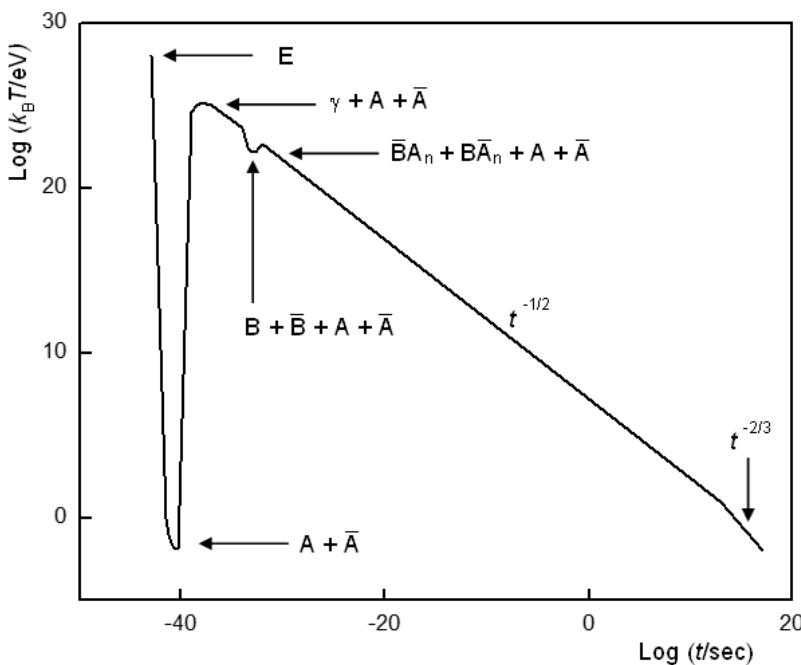
Figure 1. Creation of the fundamental particles of nature. a) First episode of inflation: the pure energy (E) of the singularity turned into a globe of A and $\overline{A}$ (reaction I). The lowest temperature is taken from ref. 4. b) First reheating: numerous annihilations of A and $\overline{A}$ raised the temperature back to what the adiabatic standard cosmology describes. While one or a small number of aether pairs annihilated into energy (reaction II), n pairs of aether, by competition, produced photons (reaction III). Some aether particles were left along and therefore survived. c) Second episode of inflation: the photons collided to create particles B and antiparticles $\overline{B}$ (reaction IV). The temperature drop in this episode is much smaller than that in the first episode. d) Second reheating: the annihilations of particles B and $\overline{B}$, without and with aether particles, raised the temperature again.

2.2. Fabric of space

Aether particles, as the fundamental units, formed vacuum[7], or the fabric of space (Fig. 2). Since they are undetectable dark matter, the nature of interparticle interaction is unknown. However, it is safe to assume that their pairs are bosons and the interaction between A and $\overline{A}$ is attractive. As it has expanded for a long time after the Big Bang, the universe cooled down to a temperature of 2.7 K. Aether particles are much lighter than atoms, corresponding to a much higher transition temperature[8], so the fabric of space has already become a Bose-Einstein condensate (BEC).

An atomic BEC could become unstable and make particles clump together[8], if the interparticle interaction is attractive. The fabric of space is different. Once a pair of A and $\overline{A}$ attract to clump or contact, the following annihilation happens:

$$A + \overline{A} \rightleftharpoons \gamma + \gamma \qquad\qquad (VIII)$$
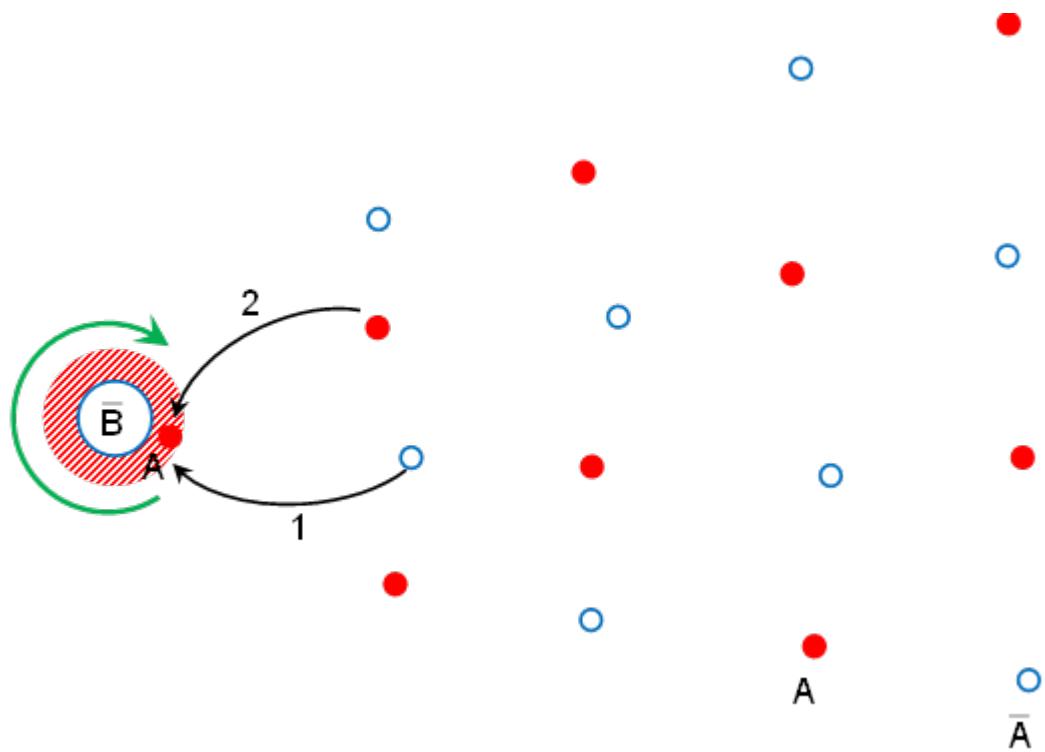
Fig. 2. A schematic diagram of a hypoatom, the fabric of space, and the generation of the sink flow of aether. Hypoatom $\overline{B}A_n$: a particle $\overline{B}$ (blue, open) is the nucleus; n particles A (slashed red area) surround the particle $\overline{B}$. Fabric of space: composed of aether particles A (red, filled) and $\overline{A}$ (blue, open). Sink flow: an $\overline{A}$ (blue, open) in the fabric of space oscillates and contacts with an A (red, filled) at the hypoatom and gets annihilated (step 1). The vacancy is then filled by another A (red, filled) in the fabric of space (step 2). The hypoatom $\overline{B}A_n$ constantly annihilates the aether particles, converting them into ultralong-wavelength photons, and thus produces a 3-dimensional sink flow of aether, warping spacetime and generating gravity. Spin of the hypoatom: the circlar motion (green) of particles A around the particle $\overline{B}$, driven by steps 1 and 2.

Since aether is the lightest particle in the universe, the generated photons are dark photons, having an ultralong wavelength, say, a light year. For reference, a reported mass[9], 8.1×10^{-23} eV, as well as other ultralight dark matter, could be a candidate of aether. The photons can penetrate across the universe, or trigger the further annihilation of other aether particles to form photons with higher energy. All these reactions are in nature the same as reaction (II); the products here are photons under the Planck distribution, which appear as the vacuum energy or dark energy. This process can be reversed to create aether particles A and $\overline{A}$ (represented as the reverse of reaction VIII).

Due to reaction (VIII), as well as the induced collective oscillations of aether particles, the velocity of a specific aether particle in the fabric of space, as Dirac has foreseen, can no longer be well defined[10]. Absolute vacuum, or the pure fabric of space, is a dynamic equilibrium system, with an equal rate of annihilation and creation of aether particles:

$$R_a = R_c \tag{4}$$

Note that the rate R_a of the annihilation is controlled by the local concentration of aether particles, while the rate R_c of the creation is determined by the energy density of the whole fabric of space, i.e. the dark energy density.

2.3. Hypoatoms

The $\overline{B}$ particles that survived from the reactions in the early universe *recombined* with aether particles A to form a species $\overline{B}A_n$:

$$\overline{B} + n A \rightarrow \overline{B}A_n \tag{IX}$$
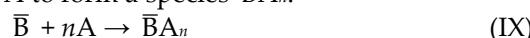
With the structure of an atom in mind, we believe that the $\overline{B}$ is a nucleus and that n A's surround the $\overline{B}$ (Fig. 2). We call $\overline{B}A_n$ a hypoatom. Note that this name does not mean that hypoatoms have the same structure as atoms. According to the particle-in-a-box model: $E_n = \frac{n^2 h^2}{8ml^2}, n \in N$, a hypoatom cannot exist as an atom, because it is impossible for the size l of a hypoatom to be much smaller than that of an atom, while the mass m and energy E_n of an aether particle are much smaller than those of an electron. Therefore, unlike the electron in an atom, the aether particle is not a standing wave in a hypoatom.

Instead, there exists a reaction on hypoatoms. An aether antiparticle $\overline{A}$ oscillating with the dark energy in the fabric of space annihilates with one of the n aether particles A of a hypoatom $\overline{B}A_n$ (step 1, Fig. 2):

$$\overline{B}A_n + \overline{A} \to [\overline{B}A_{n-1}] + \gamma + \gamma \qquad (X)$$
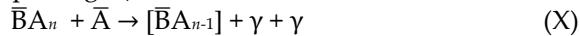
The vacancy left in the hypoatom will then be filled by a particle A from the fabric of space (step 2, Fig. 2):

$$[\overline{B}A_{n-1}] + A \to \overline{B}A_n \qquad (XI)$$

Therefore, hypoatoms $\overline{B}A_n$ constantly consume the aether particles in the fabric of space:

$$A + \overline{A} \to \gamma + \gamma \qquad (XII)$$

which is the forward of reaction (VIII), and, in nature, reaction (II). With that, the aether in a hypoatom can be regarded as a standing wave with an ultralong wavelength; hypoatoms are stabilized. Therefore, a hypoatom is not a small, localized particle. Instead, it can be regarded as an ultralarge, nonlocalized particle: a small core $\overline{B}A_n$ tied up by the aether particles in the fabric of space. The size of a hypoatom can be considered as the same as the wavelength of a dark photon, or even the same as the size of the universe.

Similarly, the survived B particles recombined with aether particles $\overline{A}$ to form an antihypoatom $B\overline{A}_n$:

$$B + n\overline{A} \to B\overline{A}_n \qquad (XIII)$$

Like hypoatoms, antihypoatoms also exist stably in a dynamic equilibrium with the fabric of space. For simplicity, antihypoatoms $B\overline{A}_n$, the antimatter counterpart of hypoatoms $\overline{B}A_n$, will not be separately discussed in this work unless necessary.

2.4. Dark energy

Based on reaction (VIII), though the interaction between A and $\overline{A}$ is attractive, the effective interaction[8] is repulsive, and hence, the fabric of space is a stable system. Compared to the momenta of the oscillations under the dark energy, the mass of an A or $\overline{A}$ is negligible: $m_A \ll q\hbar/c$, therefore the Bogoliubov dispersion relation is simplified[11]:

$$\omega = qc \qquad (5)$$

where q, $\hbar$, c, ω are wave vector, reduced Planck constant, speed of light, and angular frequency, respectively. Based on the Planck distribution, almost all of the oscillations occupy the ground state:

$$\epsilon_0 = \frac{1}{2}\hbar\omega \qquad (6)$$

Since the density of states is: $g(\omega) = Vq^2/2\pi^2 c$, by summing up all frequencies from reactions (II) and (III), we have the dark energy density:

$$\varepsilon_{vac} = \frac{1}{V}\int_0^{\omega_{A,m}} g(\omega)\epsilon_0 d\omega = \frac{\hbar\omega_{A,m}^4}{16\pi^2 c^3} \qquad (7)$$

where $\omega_{A,m}$ is the maximum angular frequency. As aether particles are oscillating in equilibrium with hypoatoms:

$$\hbar^2 \omega_{A,m}^2 = m_{\overline{B}A_n}^2 c^4 + q_{\overline{B}A_n}^2 c^2 \hbar^2 \gtrsim m_{\overline{B}A_n}^2 c^4 \qquad (8)$$

the dark energy density is

$$\varepsilon_{vac} \gtrsim \frac{m_{\overline{B}A_n}^4 c^5}{16\pi^2 \hbar^3} \qquad (9)$$

According to the Planck 2018 results[12], Hubble constant $H_0 = 67.66 \pm 0.42\ km\ s^{-1} Mpc^{-1}$, the density parameter for dark energy $\Omega_\Lambda = 0.6889 \pm 0.0056$, so the dark energy density is 5.92×10⁻²⁷ kg/m³. Therefore, the upper limit of the mass of the hypoatom is ca. 8 meV. This mass is close to that of a neutrino.

2.5. An earlier inflation

Although a wider range was proposed[13], the inflation is generally assumed in the context of the Grand Unified Theory (GUT)[2-4, 14]. However, based on the following factors: a) reaction (I) converted the pure energy of the singularity into aether particles A and $\bar{\text{A}}$; b) aether particles A and $\bar{\text{A}}$ are not included in the GUT; c) it is widely accepted that gravity begins to differentiate from the other three forces at the Planck time (discussed below), there should have been an inflation that started as early as the Planck time if not earlier (Table 1).

At the Planck time, 5.4×10^{-44} sec, the energy density of the false vacuum was 1.2×10^{19} GeV, equivalent to the mass density of $\rho_f = 5.2 \times 10^{96}$ kg/cm³. The inflation started at a patch size of the Planck length, $l_{\text{Pl}} = 1.6 \times 10^{-35}$ m. From the first-order Friedman equation: $\left(\frac{\dot{a}}{a}\right)^2 = \frac{8\pi G \rho_f}{3}$, we have the size of the universe exponentially increase in the function of $a = \text{Constant} \cdot \exp(\chi t)$, where $\chi = \sqrt{\frac{8\pi G \rho_f}{3}} = \sqrt{\frac{8\pi c^5}{3\hbar G}} = 5.4 \times 10^{43}$ sec-1. The universe after the first episode of the inflation and reheating (reactions I ~ III) would at least be as large as one half the wavelength of the B particle:

$$a \approx \lambda_{\text{B}}/2 = \frac{hc}{E_{\bar{\text{B}}\text{A}_n}} \gtrsim \frac{hc}{8 \text{ meV}} = 0.16 \text{ mm} \tag{10}$$

Thus the size of the present universe:

$$a_0 \gtrsim \frac{1.2 \times 10^{18} \text{ GeV}}{k_{\text{B}} \times 2.7 \text{ K}} \times 0.16 \text{ mm} = 9.0 \times 10^{10} \text{ light years} \tag{11}$$

which is in agreement with the inflationary theory[14].

Table 1. List of particles created in the early universe.

Time	Energy	Events	Particles created
< 10-43 s	> 10¹⁹ GeV	Symmetry breaking (gravity separated from other three forces)	A & $\bar{\text{A}}$
10-34 ~ 10-32 s	10¹⁵ ~ 10¹⁴ GeV	Electrostrong symmetry breaking	B & $\bar{\text{B}}$, or UHE neutrinos
(10-22 s)	(10⁸ GeV)	Gauge desert	Intermediates
10-12 ~ 10-6 s	100 ~ 0.1 GeV	Electroweak symmetry breaking	u, d & e
1 ~ 10 s	1 ~ 0.1 MeV		Nuclei
~ 10¹³ s	~ 0.4 eV		Atoms

2.6. Neutrinos

The next to be created, after aether particles, in the second episode of inflation and reheating were $\bar{\text{B}}$ particles (for simplicity, B particles will not be discussed). On the other hand, based on the inflationary theory[2-6, 13, 14], at ca. 10-34 ~ 10-32 sec or 10¹⁵ ~ 10¹⁴ GeV there was supposed to be a phase transition for the formation of a GUT particle (Table 1). To resonantly produce intermediate Z-bosons[15, 16]:

$$\nu + \bar{\nu} \to Z \tag{XIV}$$

if a neutrino mass eigenstate is a hypoatom: $m_\nu = m_{\bar{\text{B}}\text{A}_n} \lesssim 8$ meV, then the required energy is:

$$E_\nu = \frac{M_Z^2}{2m_\nu} \gtrsim 5 \times 10^{14} \text{ GeV} \tag{12}$$

These neutrinos at the GUT energy scale are called ultrahigh-energy (UHE) neutrinos. Therefore, UHE neutrinos and $\bar{\text{B}}$ particles were created at the same time. In addition, they both have a unique characteristic property. The neutrino cross section increases with energy[17, 18]. If we recognize each created $\bar{\text{B}}$ particle, with A particles nearby, as an ultra-large hypoatom $\bar{\text{B}}\text{A}_n$, then when the universe was cooled down, the hypoatom energy decreased with cross section.

This can further be confirmed by the phase transitions that happened in the early universe (Table 1). Up-quarks, down-quarks and electrons were created at ca 10-12 ~ 10-6

sec, nuclei at ca $1 \sim 10^2$ sec, and then nuclei and electrons recombined to form atoms at ca 10^{13} sec. Aether particles were created at ca $10^{-44} \sim 10^{-42}$ sec, and $\overline{B}$ particles at ca $10^{-34} \sim 10^{-32}$ sec. All these time slots are about $10^{10} \sim 10^{11}$ times apart, so if there were a phase transition similar to the recombination of atoms, it would be at the next time slot near 10^{-22} sec or 10^8 GeV (Table 1). However, no stable particles were created in the period of $10^{-32} \sim 10^{-12}$ sec or $10^{14} \sim 10^2$ GeV, which is called the *gauge desert*[13]. This matches our assumption: no recombination process was required to form hypoatoms; hypoatoms are neutrinos. Note that if the Z bosons decayed into photons, reaction (XIV) is equivalent to reaction (V), another agreement of our model with particle physics.

Of course the gauge desert was not truly quiet; various intermediates were formed in this period from the lepton asymmetry to the baryon asymmetry. Although the mechanism has not been fully understood, it is well accepted that flavor matters in this process. First, the third generation Yukawa couplings presented at ca 10^{12} GeV, then decayed into the second generation (ca 10^9 GeV) and finally into the first generation (ca 10^5 GeV)[19, 20]. This is understandable, because while the cross section reduced with temperature, the stability of hypoatoms that are composed of both matter and antimatter could be challenged. $10^{-32} \sim 10^{-12}$ sec can therefore be considered as the period that nature explored the stable states. Stabilized particles, which are up-quarks, down-quarks and electrons, then formed atoms. Thus our model fits in the baryogenesis-through-leptogenesis theory[19, 20].
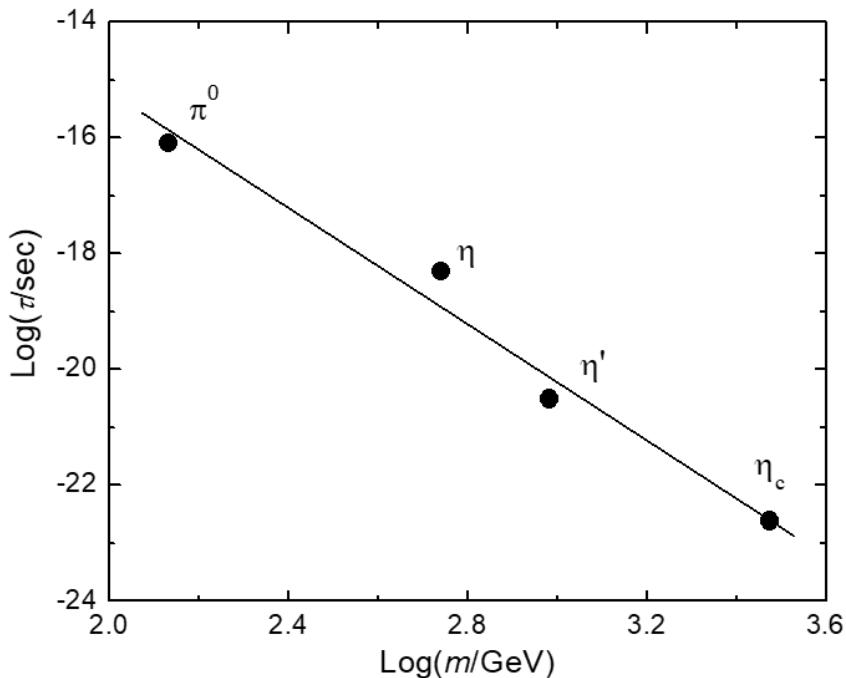
Fig. 3. A plot of the lifetimes of the pseudoscalar mesons $q\bar{q}$ composed of symmetric quark q and antiquark $\bar{q}$ versus their masses. By extrapolating the line: $\log(\tau/\text{sec}) = -5.2123 - 5.0000 \log(m/\text{GeV})$ to 8 meV, the upper limit of the mass of a hypoatom, then the lifetime would be ca 2×10^{35} sec. Based on our postulate, annihilation only happens if all of the $n+1$ bodies that form an asymmetric hypoatom contact simultaneously. Therefore, the lifetime of a hypoatom would be much longer than 2×10^{35} sec, a value projected for a 2-body meson-like particle.

2.7. Stability of hypoatoms

One might wonder how a particle composed of matter and antimatter could be stable. We will therefore discuss the lifetime of hypoatoms before any further discussion.

Known particles closest to hypoatoms $\overline{B}A_n$ are the pseudoscalar mesons that have the same amount of matter and antimatter. Based on Sargent's rule, the lifetime of a type of particle, including mesons, is directly proportional to the reciprocal of the mass to the fifth-power[21]: $\tau \propto 1/m^5$. Fig. 3 plots the lifetimes of the pseudoscalar mesons $q\bar{q}$ composed of symmetric quark q and antiquark $\bar{q}$ versus their masses[22]. If we extrapolate the line: $\log(\tau/\text{sec}) = -5.2123 - 5.0000 \log(m/\text{GeV})$ to the upper limit of the mass of a hypoatom, then the lifetime of a meson-like particle with the mass of 8 meV will be ca 2×10^{35} sec. Based on our postulate, annihilation only happens if all of the $n+1$ bodies that form a hypoatom contact simultaneously. Even if some of the n particles A settle on the particle $\overline{B}$, annihilation will not happen. Therefore, the lifetime of a hypoatom should be much longer than 2×10^{35} sec, which is projected for a 2-body meson-like particle. For comparison, the theoretical lifetime of an electron[23] is 2.1×10^{36} sec, and that of a proton[24] is in the range of $10^{35} \sim 10^{43}$ sec.

It is interesting to note that based on the above calculation, a Majorana neutrino would stably exist in a structure as $[(\overline{B}A_n)(B\overline{A}_n)]$, with an estimated lifetime of ca. 6×10^{33} sec.

2.8. Creation strategy

The matching lifetimes are not an accident. While using a type of matter particle and antimatter particle, such as A and $\overline{A}$, no stable systems would be created, using two types of matter particles and antimatter particles with significantly different masses, such as A and $\overline{B}$ or $\overline{A}$ and B, stable hypoatoms $\overline{B}A_n$ and antihypoatoms $B\overline{A}_n$ would be created. Nature uses this strategy of the asymmetric structure of hypoatoms and antihypoatoms to create this world.

Now we have a sketch of the universe: a) the fabric of space, or vacuum, is formed by aether particles A and $\overline{A}$ and their energy form; b) all observable matter particles are composed of hypoatoms $\overline{B}A_n$ (neutrinos) and antihypoatoms $B\overline{A}_n$ (antineutrinos), the enigma of missing antimatter does not exist!

It is of interest to note from its composition that a hypoatom $\overline{B}A_n$ does *own* the energy that Einstein taught us: $E = m_{\overline{B}A_n}c^2$, and it can be released once annihilated. A typical example is the nuclear energy that is released when some hypoatoms or neutrinos are annihilated in nuclear reactions.

III. DISCUSSION

3.1. General theory of relativity

In the general theory of relativity, the pure fabric of space is regarded as flat spacetime (equation 4 is valid):

$$ds^2 = -c^2 dt^2 + dr^2 + r^2 d\Omega^2 \qquad (13)$$

Based on our proposed model, the annihilation and creation of aether are in equilibrium (reaction VIII). Therefore, there is no net flow of aether particles (equation 4), and hence, aether has no observable mass in the pure fabric of space.

Now if a massive object is introduced, the rate R_a of annihilation rises dramatically. This annihilation generates a 3-dimensional *sink flow* of aether particles towards the center of the massive object. It is this sink flow that warps the spacetime in the vicinity of the massive object! Because of this flow, the time term of equation (13) needs to be rewritten with the time-dilation expression: $\sqrt{1 - v^2/c^2}\,dt$ and its radial term with the length-contraction expression: $\frac{dr}{\sqrt{1-v^2/c^2}}$, while the last term on the right stays correct[25]. Considering equation (2), we have the Schwarzschild metric (equation 1). To the best of our knowledge, this is the first *derivation* of the general theory of relativity, the greatest law of nature. If the speed of the sink flow is small, the relativistic effect is negligible; we then have Gauss's law or Poisson's equation for gravity: $\nabla^2 \phi = 4\pi G\rho$, equivalent to Newton's law of universal gravitation.

In the above analysis, the creation of aether particles (the reverse of reaction VIII), which reduces the sink flow a bit, has not been considered, because compared to that of the annihilation, the rate of the creation is negligible:

$$R_a - R_c \approx R_a \qquad (14)$$

If it is considered, then Einstein's field equation should be written with the addition of the Λ term, and Newton's law is: $\nabla^2 \phi = 4\pi G\rho - \Lambda c^2$.

With the existence of the sink flow, aether particles in the fabric of space are in fact oscillating in *quasi*-equilibrium with hypoatoms (equation 8). It is time to note that this quasi-equilibrium is natural: if the dark energy density were higher, then more aether particles would be annihilated at hypoatoms, equivalent to a higher flowrate of the sink flow, thus resulting in a larger hypoatom mass and vice versa.

Based on the Landau criterion, within the limit of the speed of light (equation 5), the fabric of space is a superfluid[7]. Therefore, the sink flow only generates the curvature of spacetime, but does not pull or push objects directly.

Interestingly, our model does show that the fabric of space has the character of negative pressure that is vital to Einstein's field equation. Think about an adiabatic cylinder-piston system. When A and $\overline{A}$ are created (the reverse of reaction VIII), the change of internal energy is: $\Delta U = mc^2$, where m is the mass of aether particles A and $\overline{A}$ created. The creation of aether particles increases the volume of the system, so the system does work: $W = p\Delta V$. According to the first law of thermodynamics, we have $mc^2 = -p\Delta V$ or $p = -\rho c^2$. When A and $\overline{A}$ are annihilated (the forward of reaction VIII), the character is identical. The negative pressure can also be understood in a different way. Each time when an $\overline{A}$ from the fabric of space annihilates with an aether particle A of a hypoatom (reaction X), the hypoatom temporarily loses, not gains, the momentum of the annihilated aether particle A. Therefore, the hypoatom experiences negative pressure.

Einstein taught us that the curvature of spacetime causes gravity, but did not mention why. Using the character of negative pressure, it is not difficult to understand gravity. For an object m under the curvature of spacetime generated by an object M, the annihilation rate on the side near M is higher than that on the far side. In other words, the force on the near side (pointing towards M) is larger than that on the far side (pointing away from M). Therefore, m experiences an attractive force, which is gravity.

Newton taught us that gravity is universal. Indeed it is, because all matter is made of hypoatoms. For the same reason, gravity cannot be shielded by any objects. The objects in the gravitational field do nothing but result in reaction (XII), further warping spacetime. This is also true for energy, which enhances the annihilation of aether particles and generates gravity, in agreement with the general theory of relativity.

The difficulty of unifying four fundamental forces is well known. Based on our model, gravity, in fact, is a collective property of aether particles in the fabric of space, while the other three forces are just interactions of the interested particles or objects.

3.2. Dark matter

For a uniform sphere M of radius r_M and density ρ_M, the rate R_a of annihilation can be calculated by the flowrate of the sink flow across the sphere of radius r:

$$R_a = 4\pi r^2 v_{esc} \rho_A \qquad (15)$$

where ρ_A is the density of the aether particles. The rate of annihilation is also proportional to mass:

$$R_a = k(M + A) \qquad (16)$$

where A is the mass of the aether particles within the sphere of radius r, and k the proportional constant, then we have

$$dA = \rho_A \cdot 4\pi r^2 dr = \left(\frac{k^2}{2G}\right)^{\frac{1}{2}} (M + A)^{\frac{1}{2}} r^{\frac{1}{2}} dr \qquad (17)$$

By integration, the mass of aether is

$$A = \left(\frac{2k^2 M}{9G}\right)^{\frac{1}{2}} r^{\frac{3}{2}} + \frac{k^2}{18G} r^3 \qquad (18)$$

and the density of aether is

$$\rho_A = \left(\frac{k^2 M}{32\pi^2 G}\right)^{\frac{1}{2}} r^{-\frac{3}{2}} + \frac{k^2}{24\pi G} \tag{19}$$

The last term on the right is the density at infinite distance ($r \to \infty$): $\rho_{A,\infty} \equiv \frac{k^2}{24\pi G}$, which is also the density in the pure fabric of space. By subtracting it, the density ρ_D of dark matter is

$$\rho_D = \rho_A - \rho_{A,\infty} = \left(\rho_M \rho_{A,\infty}\right)^{\frac{1}{2}} \left(\frac{r_M}{r}\right)^{\frac{3}{2}} \tag{20}$$

The mass D of dark matter in the vicinity of M is

$$D = 2\left(\frac{4}{3}\pi r^3 \rho_{A,\infty} M\right)^{\frac{1}{2}} \tag{21}$$

which is divergent. This indicates that all the halos in the universe are overlapping, which is correct as gravity is infinite.

To estimate the amount of dark matter, we need to choose a cutoff radius. From $-\frac{GM}{r} + \frac{1}{6}\Lambda c^2 r^2 = 0$, where $\Lambda = 8\pi G \rho_{vac}/c^2$, and ρ_{vac} is the density of dark energy, we have

$$r_{cut\text{-}off}^3 = \frac{6GM}{\Lambda c^2} = \frac{M}{\frac{4}{3}\pi \rho_{vac}} \tag{22}$$

The mass of dark matter in the vicinity of M, at least, is

$$D_{min} = 2\left(\frac{\rho_{A,\infty}}{\rho_{vac}}\right)^{\frac{1}{2}} M \tag{23}$$

The most important piece of information here is that every massive object in the universe has a dark matter halo whose mass is proportional to its own mass. Because the ratio $\rho_{vac}/\rho_{A,\infty}$ or the equilibrium constant of reaction (VIII) is unknown, we cannot compare D_{min}/M with the ratio of dark matter to ordinary matter from cosmological observation. Given the fact that most popular stellar systems are galaxies composed of stars, this proportional relation allows us to estimate the mass of the dark matter halo for a galaxy by simply summing up all the masses in the galaxy. Because stars are distributed in the galaxy, the density will reduce along the radial direction a little slower than that of an isolated object ($r^{-1.5}$, equation 20). For comparison, a profile[26] of dark matter obtained from cosmological N-body simulations has an asymptotic slope of $r^{-1.4}$. Therefore, aether is a major contributor to dark matter.

It is of interest to note that as the universe expands, the mass ratio of dark matter to ordinary matter almost stays the same (equations 21 and 23), while the mass ratio of dark energy to matter increases with the expansion because the density of dark energy is a constant. This is in agreement with the results of cosmological observation.

3.3. *Quantum mechanics*

Based on our model, quantum mechanics can be understood relatively easily. Here are a couple of examples.

Because all particles are in the fabric of space and the fabric of space is a constantly oscillating dynamic system, the wave-particle duality is natural.

The zero-point vibration of aether particles (equation 6) is equivalent to Heisenberg's uncertainty principle.

In theory, particles heavier than aether could be created by multiple ultralong-wavelength photons. Of course, the heavier the particles, the lower the chance of creation, corresponding to a shorter lifetime in the quantum field theory.

The wave function of a particle from the Schrodinger equation is the superposition of wave vectors from the local interactions and the creation and annihilation (reaction VIII) of aether particles in the fabric of space, not a property of only the interested particle itself. This is why Lorentz invariance is violated for Schrodinger's wave functions.

For the double-slit interference experiment, the interference pattern of electrons (or photons) is obtained because the oscillation of the local fabric of space is interfered by the slits. When they are *observed*, the light of observation overwrites the interfered fabric of

space, or the so-called wave function collapse occurs, hence the interference pattern no longer exists.

In order for the system of an object that is held by our hand, as well as our arm, to return to its original state, the system must rotate two cycles (i.e. 720°). Similarly, hypoatoms are held by the fabric of space (Fig. 2) and have to rotate two cycles to return to the original quantum state. Therefore, it is natural that hypoatoms are spin-1/2 particles. When they have additional symmetry, particles made from hypoatoms would have different spin characters.

As shown in Fig. 2, reaction (XII) is also the origin of the angular momenta of hypoatoms. Since reaction (XII) always exists, hypoatoms rotate constantly. The angular momentum will never disappear and hence becomes the intrinsic property of a hypoatom.

Furthermore, standing waves of aether can exist between hypoatoms, which leads to the entanglement of particles (Fig. 4). Once one of the particles is observed, the standing wave between them is overwritten. Therefore, the entangled system collapses into a pair of particles that are spinning in opposite directions. The inflations in the very early universe and the falling fabric of space within a black hole (discussed below) indicate that there is no speed limit on the motion of aether. We thus suspect that there would be no speed limit on the collapse of an entangled system.

The Stern-Gerlach experiment can also be understood easily. Under the external magnetic field in a Stern-Gerlach apparatus, hypoatoms or those made from them are forced to spin either up (+) or down (-). We can understand this by imagining that when it is placed on a watershed, water flows down either towards the north or the south. For an apparatus S, 50% of the hypoatoms will go through $\left\{ \begin{smallmatrix} + \\ -| \end{smallmatrix} \right\}_S$ or $\left\{ \begin{smallmatrix} +| \\ - \end{smallmatrix} \right\}_S$ (Feynman's symbol, ref.[27]).
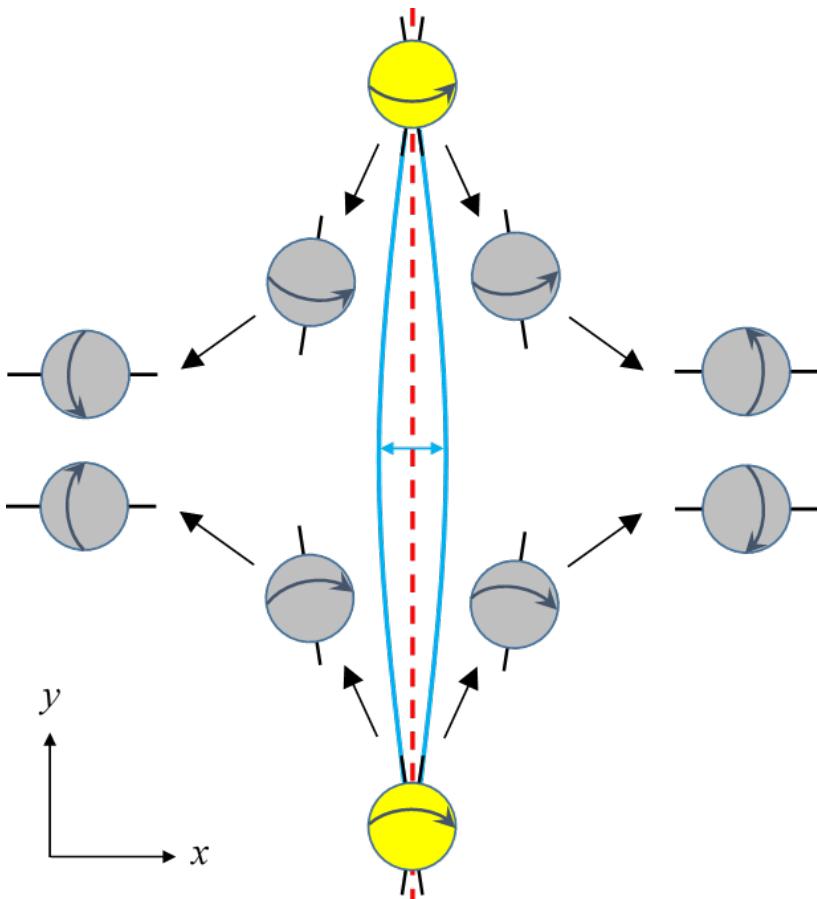
Fig. 4. A schematic diagram on the entanglement of particles. A standing wave (blue, solid curves) exists between two entangled particles (yellow). Once one of the particles is observed, the standing

wave between them is overwritten. Therefore, the entangled system collapses into a pair of particles that are spinning in opposite directions (grey). The dashed line (red) between the entangled particles is a watershed.

If we have two apparatuses S in succession $\left\{{+\atop-|}\right\}_S \left\{{+\atop-|}\right\}_{S'}$ 100% of the hypoatoms that go through the first go through the second. If we have $\left\{{+\atop-|}\right\}_S \left\{{+|\atop-}\right\}_{S'}$ none of the hypoatoms that go through the first can go through the second.

If we tilt the second apparatus T by 90° (ref.[27]), then when the hypoatoms that go through the first reach the second, they are in fact, once again, placed in a watershed-like potential field and forced to spin either left (+) or right (-), just like when they encountered the first apparatus. Therefore, for either the experiment $\left\{{+\atop-|}\right\}_S \left\{{+\atop-|}\right\}_T$ or $\left\{{+\atop-|}\right\}_S \left\{{+|\atop-}\right\}_T$, only 50% of the hypoatoms that go through the first can go through the second.

Similarly, for the experiment $\left\{{+\atop-|}\right\}_S \left\{{+\atop-|}\right\}_T \left\{{+\atop-|}\right\}_{S'}$ the hypoatoms are placed in a watershed-like potential field at the third apparatus. The hypoatoms spinning left (+) that pass the second are forced to spin either up (+) or down (-) again. There is no reason that they should remember their spin directions when they pass the first apparatus. They do not remember any history, thus only 50% of those passing the second can go through the third.

Because hypoatoms are the fundamental building blocks, particles made from them can also have properties discussed as above.

Another unsolved problem is the conflict between the general theory of relativity and quantum mechanics. For a massive object, as the size goes down, for example, to the Schwarzschild radius, quantum effects from the dynamic fabric of space become negligible. Therefore, the general theory of relativity and quantum mechanics are compatible.

3.4. Black hole

The most condensed star that can be directly observed is a neutron star. If its mass further increases, it collapses into a black hole. Within a black hole, it is generally believed to form a singularity. However, based on the proposed hypoatom structure, hypoatom degeneracy pressure can provide new support to prevent the collapse. In other words, the core of a black hole within the event horizon would be a hypoatom star or a neutrino star.

Outside its event horizon, a rotating black hole usually has an accretion disk perpendicular to the axis of rotation. As we have known, the accretion plane is the primary direction that matter falls into the black hole. Although we do not exactly know the physical law inside the event horizon, it is reasonable to assume that matter from the accretion disk would continue to fall (faster than the speed of light) into the core of the black hole in spiral flows $\mathbf{V}_s$. Fig. 5 illustrates the structure of a black hole. As the falling fabric of space passes through the event horizon, the photons from the annihilation of aether could no longer escape. The dark energy density inside the event horizon would thus be increased; there would exist a fireball. This annihilation process would easily become a nonlinear system, leading to pulsations or the so-called quasi-periodic oscillation[28].

The raised dark energy density would break the equilibrium with hypoatoms (equation 8). Therefore, it would initiate reaction (IV), creating B particles or, in consequence, hypoatoms. Together with the falling matter, if it exists, this process makes the mass of the hypoatom star increase or the black hole grow. The creation of hypoatoms or neutrinos would be the primary ability of black holes in the evolution of nature. This mechanism to create hypoatoms within black holes would be identical to the particle creation mechanism in the early universe, i.e. reactions (III) ~ (VII).

At the Big Bang, the universe was only able to convert part of its energy into matter by zigzagging inflation and reheating processes (reactions I ~ VII, IX and XIII). Therefore, it is reasonable to assume that in a much milder process on the course of the growth of black holes, not all aether falling into black holes would immediately be converted into

hypoatoms and immobilized at the core. The energy that is not immobilized would temporarily escape from the core as emission beams V_b along the magnetic axis of the core (Fig. 5). Of course nothing would be able to escape beyond the event horizon; the V_b would fall back as back falling flows V_f for further conversion and immobilization. The V_f would exist in two ways: a) immediately surrounding the V_b, and b) eventually falling into the V_s plane (Fig. 5). This scene of a neutrino star inside a black hole would be similar to that of a pulsar, its less dense counterpart[29].
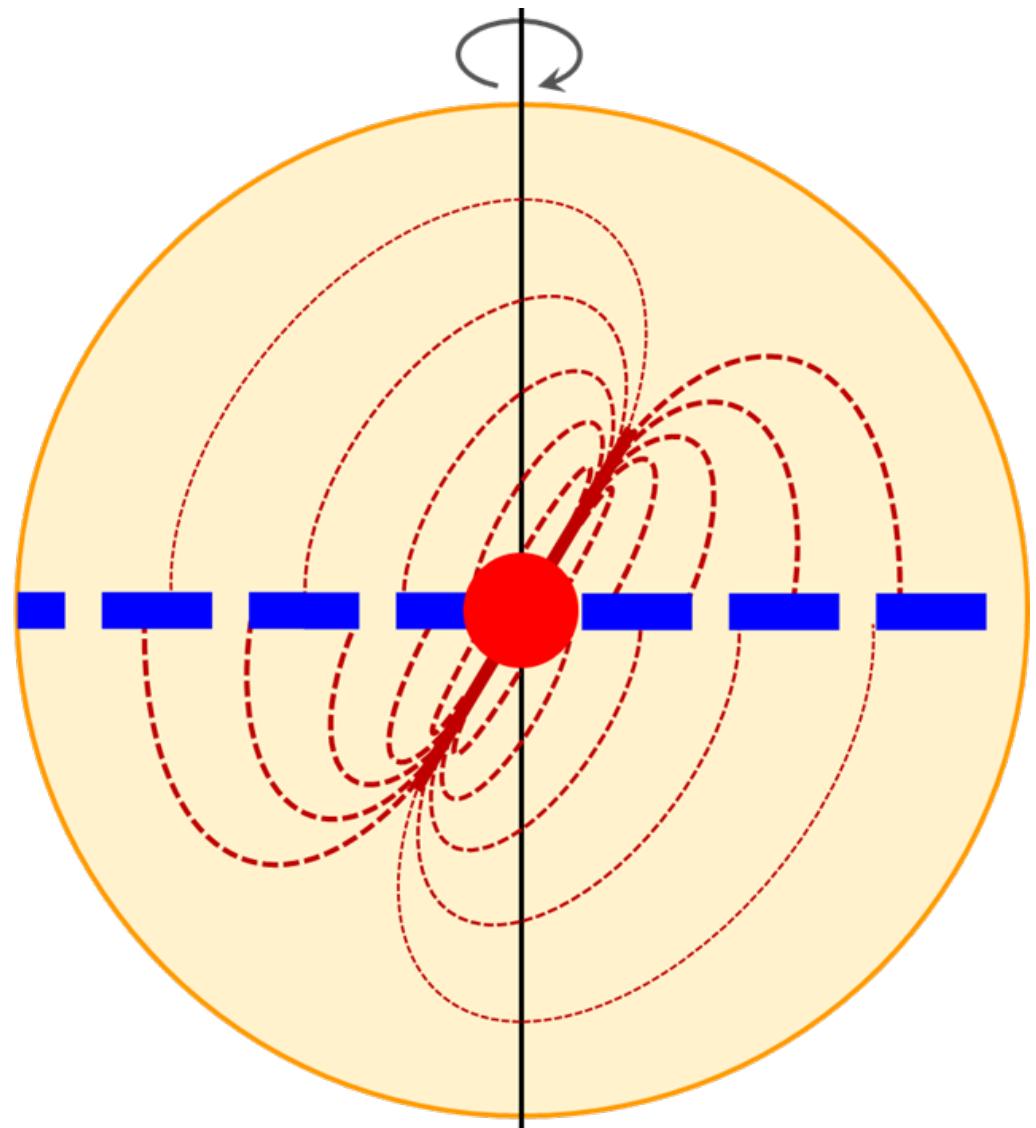
Fig. 5. A schematic diagram of a black hole. The circle (yellow) is the event horizon. The center (red) is a neutrino star. The vertical line (black) is the axis of spin. The horizontal zone (blue) represents the falling spiral flows, going in on the left and coming out on the right. The slashed lines (dark red) are the emission beams, emitting along the magnetic axis from the neutrino star (red). The dashed curves (dark red) represent the back falling flows (the thicker the curves, the larger the possibilities), either immediately surrounding the beams (dark red) or further into the spiral plane (blue). The filling (light yellow) within the event horizon (yellow) is a lit fire due to the annihilation of the fabric of space.

3.4.1. Birth of the universe

Analogous to the Tolman-Oppenheimer-Volkoff limit for neutron stars, we can estimate a mass limit for a neutrino star or a black hole:

$$M \approx \left(\frac{m_\mathrm{n}}{m_\nu}\right)^2 M_\mathrm{n} \gtrsim \left(\frac{939.6\ \mathrm{MeV}}{8\ \mathrm{meV}}\right)^2 \times 2.2 M_\odot = 3 \times 10^{22} M_\odot \qquad (24)$$

where m_n is the mass of a neutron, m_ν the mass of a neutrino, M_n the mass limit of a neutron star, and $M_\odot$ the mass of the sun. Another method to estimate the mass limit for a neutrino star is to calculate the Jeans mass of the neutrino[30]:

$$M = \frac{1.8 M_\mathrm{Pl}^3}{m_\nu^2} \gtrsim \frac{1.8 \times (1.22 \times 10^{19}\,\mathrm{GeV})^3}{(8\ \mathrm{meV})^2} = 5 \times 10^{22} M_\odot \qquad (25)$$

where M_Pl is the Planck mass. Without considering a potential addition due to the rotation of the black hole, both lowermost values estimated from the uppermost mass of neutrino are very close to the accepted mass of the observable universe, ca. $10^{23} M_\odot$. If the mass of a black hole exceeds this limit, the structure of the hypoatoms cannot withhold and thus the black hole or neutrino star collapses. In result, all particles annihilate to become the pure energy that is named as a singularity, in which the wavelength of photons is asymptote to zero. Thus the black hole turns into a white hole, producing the Big Bang (Fig. 6).
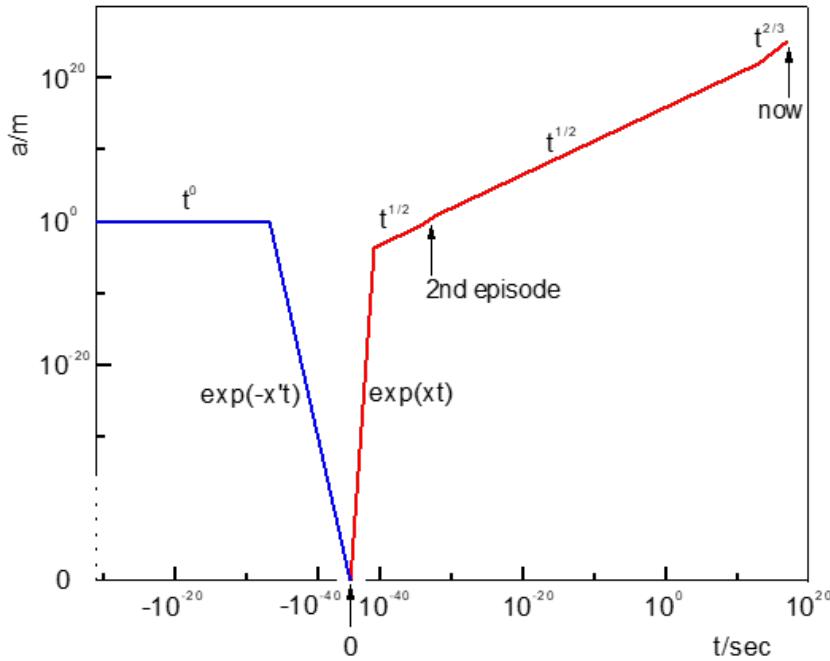
Fig. 6. The size of a universe before and after a Big Bang. Before the Big Bang (blue): it is a growing black hole. At ca. $10^{-34} \sim 10^{-32}$ sec before the Big Bang when its mass exceeds ca. $3 \times 10^{22} M_\odot$, the core of the black hole collapses from ca. 2 m into a singularity. After the Big Bang (red): the universe expanded with zigzagging inflation and reheating processes, creating the fundamental particles of nature. After the first episode of inflation and reheating at ca. 10^{-41} sec, the size of the universe is ca. 0.25 mm. After the second episode of inflation and reheating at ca. $10^{-34} \sim 10^{-32}$ sec, the universe returns to its size before the collapse.

The lowest cross section of neutrinos experimentally measured[31] is about 10^{-56} cm². If we use it to estimate the density of the hypoatoms: $\rho_\nu = 8\ \mathrm{meV}/(10^{-30}\ \mathrm{m})^3 \sim 10^{52}\ \mathrm{kg}/m^3$, then the minimum size of the cores of black holes right before the collapse can be estimated: $a \sim \sqrt[3]{M/\rho_\nu} \gtrsim \sqrt[3]{3 \times 10^{22} M_\odot / 10^{52}} = 2$ m. This collapse before the Big Bang can almost be regarded as the reverse process of the inflation after the Big Bang (Fig. 6).

Interestingly, the first episode of the inflation (reaction I) was a process to create, not consume, aether particles A and $\bar{\mathrm{A}}$. Therefore, the gravity during the inflation appeared

as a repulsive force! Although producing an attractive gravity later on, A and $\bar{\text{A}}$ in the inflation were a repulsive-gravity material. Based on earlier discussion, this process did produce negative pressure. This mechanism is in agreement with the inflationary theory[14]. On the other hand, gravity indeed is the first force separated with the GUT force or from the universal forces, because once reaction (I) occurred, gravity existed. While they formed the matter of the universe, created B particles reduced the gravity of the universe, such that the universe would not collapse back to a black hole.

3.4.2. Where we are

Based on our model, right before the Big Bang, the precursor black hole of our universe, a hypoatom star or neutrino star, collapsed into a singularity that can be regarded as photons whose wavelength is asymptote to zero. The singularity then turned into a white hole, emitting matter and energy at the speed of light or higher, which is the Big Bang. We have known that before the collapse, besides the falling fabric of space, there existed the falling spiral flows $\mathbf{V}_s$, the emission beams $\mathbf{V}_b$ and the back falling flows $\mathbf{V}_f$ around the core of the precursor black hole (Fig. 5). These flows would be essential for the precursor neutrino star to grow and reach the mass limit for the Big Bang at ca. $10^{-34} \sim 10^{-32}$ sec before the Big Bang (Fig. 6). Although their generations would be interrupted during the short emitting moment of the white hole, the $\mathbf{V}_s$ and $\mathbf{V}_f$ flows would exist after the Big Bang, so would the $\mathbf{V}_b$ beams due to the momenta they had in the precursor black hole. All of these flows would certainly interact with the powerful radial expansion waves $\mathbf{V}_{BB}$ of the Big Bang (Fig. 7).

Because the $\mathbf{V}_s$ flows were perpendicular to the $\mathbf{V}_{BB}$, they collided, resulting in hot spirals in the infant universe, even though the momenta of the $\mathbf{V}_s$ were small compared to that of the $\mathbf{V}_{BB}$. The hot spirals intersected with the surface of last scattering (SLS) generating a hot ring in the cosmic microwave background (CMB). Half of the hot ring is easily noticeable in the range from Galactic coordinates $(l, b) \sim (265°, 20°)$ to $(100°, -15°)$ in the CMB[32], which is often related to the *Axis of Evil*. The hot ring is super thick, with an open angle larger than $30°$ in the CMB, but is not always continuous, which is reasonable as it originated from the $\mathbf{V}_s$. The hottest points in the middle of the ring, labelled as 1 to 9 (Fig. 7a), are taken to define the $\mathbf{V}_s$ plane. The standard deviations of reading the Galactic coordinates from multiple Planck CMB maps[32]: SMICA, Commander, NILC, SEVEM, SMICA-NOSZ, and Fgsub-sevem, are less than $1°$. If we convert the Galactic coordinates into the Cartesian coordinates, then the best-fit $\mathbf{V}_s$ plane that can best represent the hot ring is:

$$z = (-0.58 \pm 0.10)x + (0.03 \pm 0.03)y - (0.36 \pm 0.06)r_{\text{SLS}} \qquad (26)$$

where r_{SLS} is the radius of the SLS.
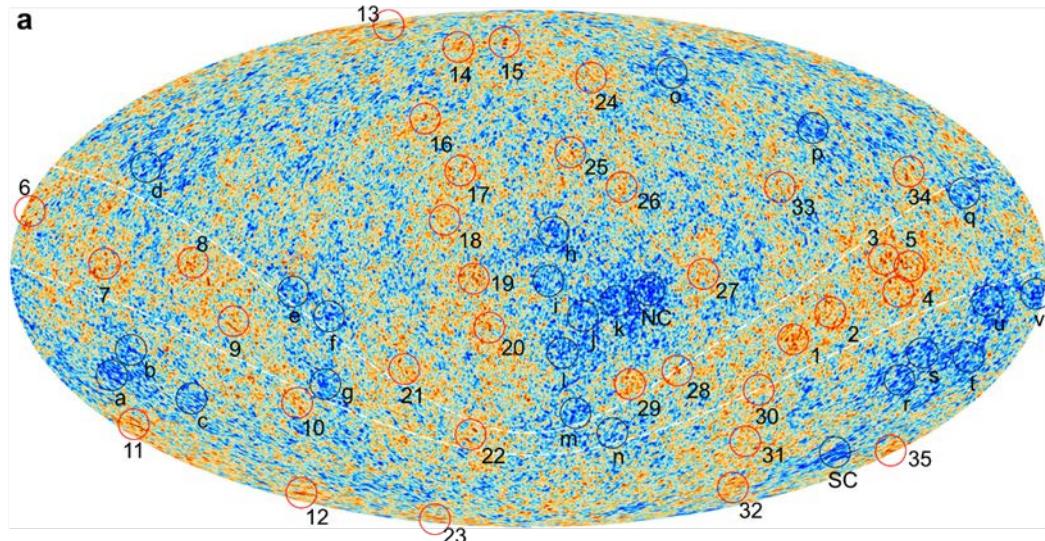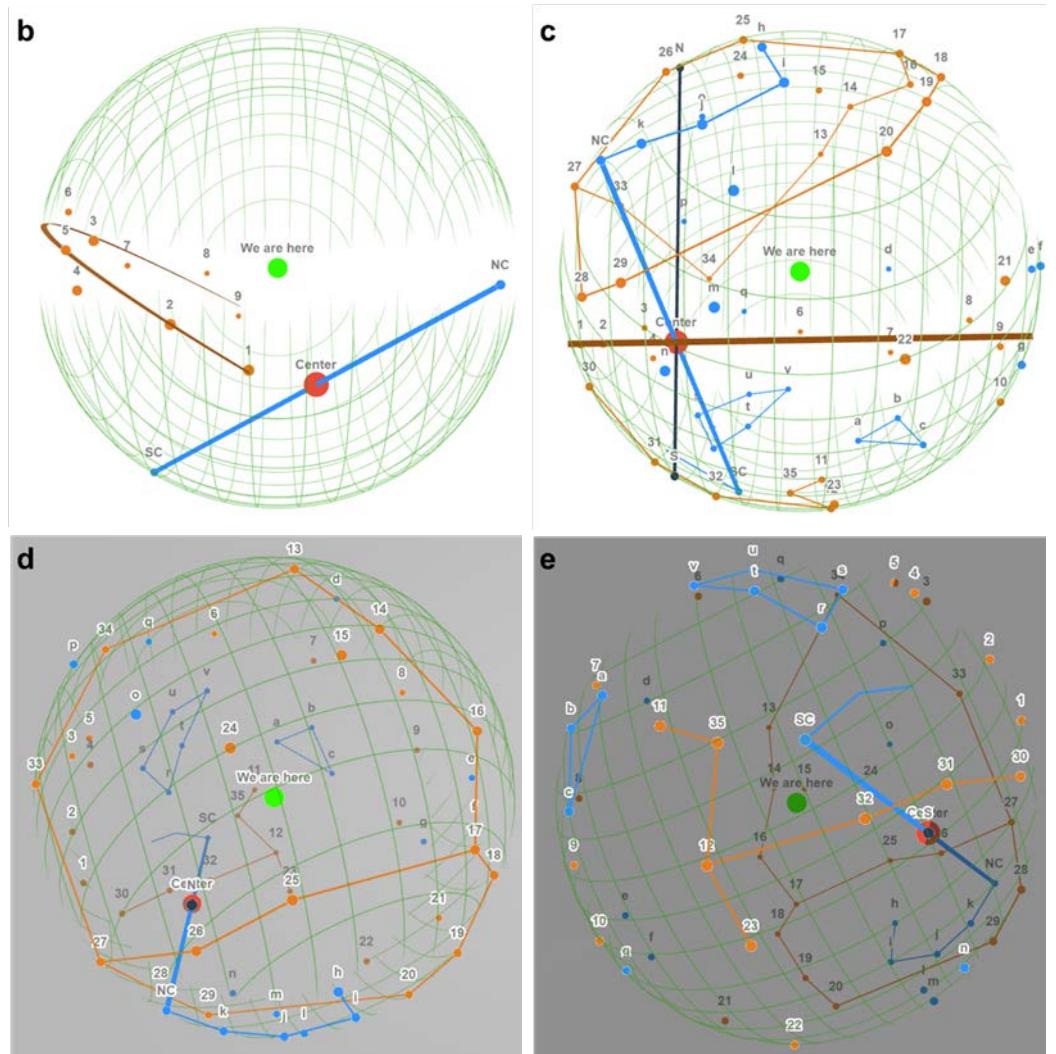
Fig. 7. The center of the universe. The lines in this figure are for guidance only. **a**, Hot (red, number) and cold (black, letter) spots are labelled in the CMB. The zone between the white dashed curves is a hot ring. **b**, 3D globe of the SLS (green), on which half of the hot ring (dark red), 1-2-3&4-5-6-7-8-9, is visible. The plane of the hot ring and the line (blue) between the SC and NC (blue) intersect at the center of the universe (red). If we look from the Local Group (green), the universe is spinning clockwise. The plane of the hot ring is the equator plane, and the Local Group is inside the North half-ball. **c**, The axis of spin is the line (black) between the N and S (black), perpendicular to the equator (dark red). The observed angle between the equator plane and the beams (blue) is ca. 58°. With this angle, the rotating precursor black hole dragged the beams (blue) to sweep. On the Northern hemisphere, a low-temperature tail, NC-k-j-i-h, is following the cold spot NC. The regions immediately surrounding the Northern beam, 29-28-27-26-25-17-18-19-20, show higher temperatures. **d**, The North half-ball, looking from the N (black). Higher temperatures are close to the edge of the Northern hemisphere, 33-34-13-14(15)-16, together with those surrounding the beam. The space below them is uniform. **e**, The South half-ball, smaller than the North half-ball. The regions immediately surrounding the beam, 35(11)-12(23)-32-31-30, show higher temperatures. The regions immediately close to the hot equator, u-s-r-t-v and a-b-c, have lower temperatures. The thin blue line from the SC shows the position of a tail if it exists.

Because the V_b had the same direction as the V_{BB}, compared to other regions (with the falling vacuum), less collisions happened, leading to a lower temperature where the V_b passed through. Therefore, two cold spots are observed in the CMB: SC, at $(l, b) = (208°, -56°)$, on the South[33] of the V_s plane, and NC, at $(l, b) = (318°, -5°)$, on the North (Fig. 7a).

We therefore have the following important results:

The $\mathbf{V}_s$ plane of the hot ring and the $\mathbf{V}_b$ axis determined by the cold spots intersected at $(l, b) = (286° \pm 10°, -43°^{+7°}_{-6°})$ and at a distance $(0.66^{+0.03}_{-0.01})r_{\text{SLS}}$ away from where we are (hereafter represented by the Local Group). This intersection is the point where the Big Bang happened or the center of the universe (Fig. 7b). Since the comoving radius of the SLS is 14 Gpc (ref.[34]), the center of the universe is 9.3 Gpc or 30 billion light years away from the Local Group.

Only half of the hot ring is observed, while the other half is hardly visible (Fig. 7a). This is due to the Doppler effect and the Doppler beaming: if we look from the Local Group, the $\mathbf{V}_s$ flows were spiraling clockwise into the precursor core of the universe. Due to the frame-dragging effect, the core also rotated clockwise. We therefore know that: a) if we look from the Local Group to the center of the universe, the universe is rotating or spinning clockwise; b) the plane of the hot ring is the plane of the equator of the universe (equation 26); c) the angle between the equator plane of the universe and the Galactic plane is $30° \pm 5°$; d) the North half-ball, or more accurately, the North half-ellipsoid, of the observable universe is bigger than the South half; e) the Local Group is inside the North half-ball; f) the axis of spin of the universe, perpendicular to the equator plane, is:

$$(x, y, z) = (0.13r_{\text{SLS}}, -0.47r_{\text{SLS}}, -0.45r_{\text{SLS}}) + (0.58, -0.03, 1.00)t \quad (27)$$

g) the spin axis intersects with the SLS at $(l, b) = (325°, 31°)$ on the North end and $(l, b) = (256°, -62°)$ on the South end.

This clockwise spin is confirmed by the cold spots and a tail in the CMB. The angle between the $\mathbf{V}_s$ plane and the $\mathbf{V}_b$ axis is $58° \pm 6°$. With this angle, the rotating precursor core dragged the beams to sweep the inner space within the event horizon, just like a pulsar sweeps through space. Therefore, a low-temperature tail spreading in a wide range is observed following the NC in the CMB (NC-k-j-i-h, Fig. 7c). A similar tail should also exist following the SC. However, the regions of the SLS that the two beams were sweeping are very different. As the Northern beam swept from h to i, j, k, and NC, the distance to the universe center reduced (Fig. 7c). This is very suitable for the tail to be observed, because the sweeping beam arrived at the SLS at almost the same time. On the contrary, as the Southern beam swept, the distance of the SLS to the universe center increased quickly (Fig. 7c). Any potential tail would thus fly beyond the SLS. In addition, the potential tail, even if it existed, would be very much overshadowed by the high temperature near the universe center and the equator.

Finally, almost all the other characters in the CMB can be explained by our mechanism. The regions immediately surrounding the $\mathbf{V}_b$ show higher temperatures (the Northern: 29-28-27-26-25-17-18-19-20, Figs. 7c and 7d; the Southern: 35(11)-12(23)-32-31-30, Fig. 7e), due to the $\mathbf{V}_f$ surrounding the $\mathbf{V}_b$. Other regions that show higher temperatures are close to the edge of the Northern hemisphere (33-34-13-14-16, Fig. 7d), due to the $\mathbf{V}_f$ falling towards the equator plane. Geometrically, the $\mathbf{V}_f$ flows also look longer and hence brighter on the edge. On the contrary, due to the lack of the $\mathbf{V}_f$, the vast region below 20-19-18-17-16-14-13-34 (Fig. 7c) is very uniform. The temperatures are lower for those close to the axis of spin rotating faster in the front, such as the l, m, and n regions (Fig. 7c), and for those rotating slower in behind, such as the r-s-u-v-t and a-b-c regions (Fig. 7e), due to the Doppler effect. For the regions immediately close to the equator from the South side (a-b-c and r-s-u-v-t), there existed an additional effect: the super thick spirals that originated from the $\mathbf{V}_s$ at the equator decoupled later because they were hotter, and hence were not as transparent as other regions.

It should be emphasized that since the universe spins, the cold spots that are used to define the $\mathbf{V}_b$ axis and, consequently, the center of the universe must be synchronous. Without the parameters inside the precursor black hole, the traditional method of using physical laws to deduce the properties of interest is invalid. We checked the distances from the cold spots to the center of the universe and found that they are the same: $(0.74 \pm 0.12)r_{\text{SLS}}$ for the NC versus $(0.76 \pm 0.12)r_{\text{SLS}}$ for the SC, therefore our results are reasonable. The Eridanus supervoid is generally believed to be insufficient to cause the temperature depression at the cold spot SC, though a recent Dark Energy Survey reported a much

stronger Integrated Sachs-Wolfe imprint[35]. Our neutrino star mechanism provides an additional explanation on the temperature depression.

Based on the Gödel metric, an exact solution of the Einstein field equations, matter in the universe rotates with the angular velocity: $\omega = 2(\pi G \rho)^{\frac{1}{2}}$, where ρ is the density of matter and G Newton's gravitational constant[36,37]. However, as Hawking emphasized, a velocity like this is a very high limit, corresponding to the order of the speed of light at a distance of the Hubble radius[38]. If the universe spun at this high angular velocity, the required centripetal force would be comparable at the present time to gravity[38]. Our neutrino star mechanism does not provide any real structures with heavy mass at the center of the universe after the Big Bang (for comparison, the precursor black hole had a heavy neutrino star core before the Big Bang). Without having sufficient centripetal force, matter has been flying away from the axis of spin. While the angular momentum is conserved, the energy of rotation has been gradually converted into that of rotationally radial expansion. Of course the dominating expansion has been accelerating (driven by the vacuum energy) in the Big Bang radial direction from the center of the universe. Therefore, we conclude that matter in the universe has been expanding in spiral trajectories.

The Local Group rotates about the axis of spin (equation 27) on the plane parallel to the equator: $z = -0.58x + 0.03y$, thus the tangential velocity component of rotation points towards $(l, b) = (39°, -23°)$. The velocity component in the rotationally radial direction $(l, b) = (121°, 18°)$ is close (with an angle of 26°) to the Big Bang radial direction $(l, b) = (106°, 43°)$, and hence can be contributed to the Big Bang radial expansion.

3.4.3. Anisotropic universe

While Lamaître and Hubble discovered an expanding universe[39,40] in the 1920s, Gamow[41] and Gödel[36,37] suspected that the universe is rotating in the 1940s. To date, the universe is generally believed to be isotropic and homogeneous; questions like where the Big Bang happened are meaningless. There has been little knowledge on whether the universe is truly rotating[38] or what the universe is rotating about.

It is important to note that the universe was born to be isotropic and homogeneous (except for its edge, of course), as it was a uniform globe of aether particles (reaction I) or hypoatoms (reactions IX and XIII). For the infant universe at ca. 380,000 years after the Big Bang, the deviation from the isotropy was insignificant. This is why the CMB looks nearly isotropic and homogeneous. As it expands, the universe has been becoming more anisotropic and nonhomogeneous, due to the vacuum energy from the edge of the universe and the spin of the universe.

We will provide multiple independent evidence from cosmological observations. The first evidence is about the spin of the universe. Other than Gödel's[36,37] and Hawking's[38] theoretical work, Longo[42] focused on spiral galaxies, an idea closer to Gamow's[41]. By counting the numbers, he found more left-handed spirals than right-handed ones, and thus believed that there is a parity violating asymmetry in the universe[42]. The axis of the dipole asymmetry was reported at $(l, b) = (52°, 68.5°)$, with an angle of 24° to equation (27), but the direction of rotation was not discussed. Shamir also found a similar asymmetry of spiral galaxies[43]. By studying quasar polarization vectors, Hutsemékers *et al*. found that the polarization angle is rotating clockwise with increasing redshift in the North Galactic hemisphere and counterclockwise in the South one, which could be interpreted by the rotation of the universe[44].

The second evidence is about the existence of the bulk flow of the local universe[45,46]. If the isotropic Hubble flow is not considered, then the local galaxy groups and clusters are moving with the Local Group. However, what we detect are their velocities in the past. Since the universe has been expanding in acceleration, the past local galaxy groups and clusters were moving slower than the current Local Group. Therefore, relative to the Local Group, the local galaxy groups and clusters appear to move backwards, which is observed as the bulk flow or dark flow. Cosmological observations are performed in the existence

of the Hubble flow. The velocity components of the galaxy groups and clusters in the transverse direction (centered at the Local Group) are difficult to detect[38] and hence insignificant to the direction of the bulk flow. After the Hubble flow is removed from the cosmological results, the observed anisotropic motion of the Local Group becomes further away from the Big Bang radial direction, and the observed bulk flow is about the opposite direction, such as $(l, b) = (254°, -19°)$ (Fig. 8a). Due to different relative positions to the Local Group, the observed direction (and magnitude) of the bulk flow must be relatively scattered, consistent with previous studies (e.g. fig. 3 in ref.[45], and fig. 13 in ref.[47]).

The ΛCDM model predicts that the bulk flow exists with a reducing speed as the distance increases, which becomes negligible farther than 400 Mpc (refs.[46,48]). Our mechanism predicts that the speed of the bulk flow increases as time goes further back, or the distance r to the Local Group increases: $|\mathbf{v}_{BF}| = C_{BF}r$, where C_{BF} can be a constant in the local universe. The observed speed of the bulk flow is about 800-1000 km/s at 400 Mpc (refs.[46,49]), corresponding to a constant $C_{BF} = 2.0 - 2.5$ km s^{-1}Mpc^{-1}. It is also worthy to note that based on our mechanism, the observed bulk flow does not mean that the local galaxy groups and clusters are truly departing from us (of course the Hubble flow still exists). This is probably why some reports reported no bulk flow[48,50].

The third evidence is about the anisotropy of the Hubble constant[47,51]. For convenience of discussion, space can be divided into four quadrants by the line between the Local Group and the center of the universe, and the tangential direction of rotation of the Local Group (Fig. 8b). The velocity of the Local Group, as well as the galaxy groups and clusters, is: $\mathbf{v} = \mathbf{u}_{rad} + \mathbf{v}_{rot}$, where $\mathbf{v}_{rot}$ is the decelerating tangential velocity component of rotation. The accelerating radial velocity component $\mathbf{u}_{rad}$ is the sum of the isotropic velocity component $\mathbf{v}_{iso}$ and the accelerating radial velocity component $\mathbf{v}_{rad}$: $\mathbf{u}_{rad} = \mathbf{v}_{iso} + \mathbf{v}_{rad}$. The typical velocity components of the galaxy groups and clusters: $\Delta\mathbf{u}_{rad} = \mathbf{u}_{rad, GG} - \mathbf{u}_{rad, LG}$ and $\Delta\mathbf{v}_{rot} = \mathbf{v}_{rot, GG} - \mathbf{v}_{rot, LG}$, are shown relative to the motion of the Local Group. For the galaxy groups and clusters in the local universe ($z \leq 0.1$), the speeds (not the direction) of rotation can be considered approximately the same as that of the Local Group: $|\mathbf{v}_{rot, GG}| \approx |\mathbf{v}_{rot, LG}|$ (alternatively, the momenta of rotation or the angular velocities can be considered approximately the same). Therefore, the anisotropy of the Hubble constant has a quadrupole character: quadrants III and I host lower Hubble constants, while quadrants IV and II host higher Hubble constants (Fig. 8b, the inner yellow circle). This quadrupole anisotropy matches what was observed by Migkas *et al.* (e.g. figs. 6 and 21 in ref.[51]). For the galaxy groups and clusters far away from the Local Group, their velocity components $\mathbf{v}_{rot, GG}$ of rotation were higher (pointing more to the right in Fig. 8b, the outer pink circle) in the past. Therefore, the Hubble constants in quadrant I increase and those in quadrupole II decrease. The anisotropy shows more dipolar character at higher z, matching the observed results[47].

For further comparison, we performed a proof-of-concept simulation (see Methods) on the anisotropy of the Hubble constant in the local universe ($z \leq 0.1$). Since the distance $\mathbf{R}$ to the center of the universe ascends more rapidly than the $\mathbf{v}_{rad}(\mathbf{R})$, the Hubble constant $H_0 = \mathbf{u}_{rad}(\mathbf{R})/\mathbf{R}$ always descends and will be asymptote to a constant. The Hubble law can be written as:

$$\mathbf{u}_{rad}(\mathbf{R}) = H_{0, iso}\mathbf{R} + \mathbf{v}_{rad}(\mathbf{R}) \tag{28}$$

where $H_{0, iso}$ is the Hubble constant that represents the isotropic expansion. For the rotation about the axis of spin (equation 27), since what we detect are the past galaxy groups and clusters, we need to add a distance term:

$$|\mathbf{v}_{rot, GG}| \approx |\mathbf{v}_{rot, LG}| + C_{rot}r \tag{29}$$
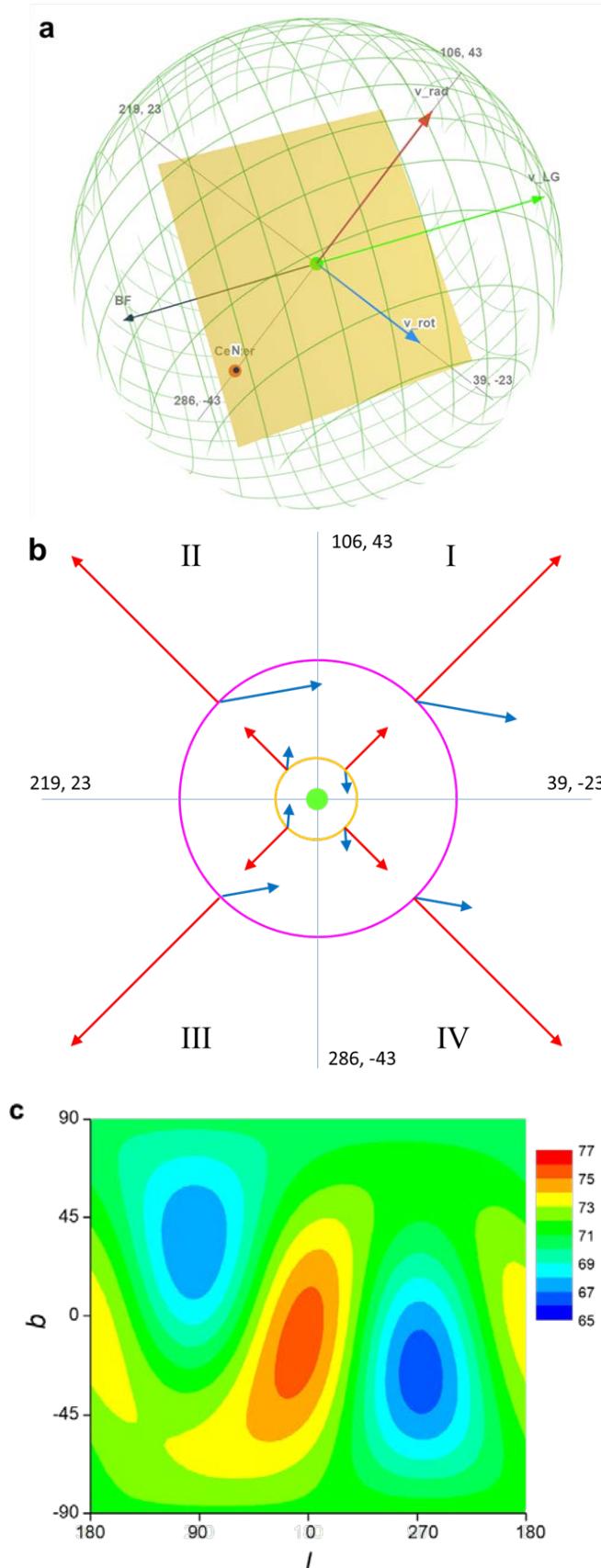
Figure 8. The anisotropic universe. a, Inside the SLS (green gridlines), the Local Group (green) rotates about the axis of spin (black, perpendicular to the paper) on the plane (yellow) above the center of the universe (red). The rotation $\mathbf{v}_{\text{rot}}$ points towards $(l, b) = (39°, -23°)$ (blue). The Big Bang radial direction $\mathbf{v}_{\text{rad}}$ points towards $(l, b) = (106°, 43°)$ (red). The anisotropic motion $\mathbf{v}_{\text{LG}}$ of

the Local Group (green) points towards the combined direction of $\mathbf{v}_{\mathrm{rot}}$ and $\mathbf{v}_{\mathrm{rad}}$, such as $(l, b) = (74°, 19°)$ (calculated from the parameters that we assumed for the simulation: $\mathbf{v}_{\mathrm{rad}} = 53{,}000$ km s^{-1} and $\mathbf{v}_{\mathrm{rot}} = 38{,}000$ km s^{-1}). The bulk flow (not to scale) points towards the opposite direction, $(l, b) = (254°, -19°)$ (black). **b**, The space anisotropy of the Hubble constant. Space is divided into four quadrants by the line between $(l, b) = (286°, -43°)$ and $(106°, 43°)$ and the line between $(l, b) = (219°, 23°)$ and $(39°, -23°)$. The typical velocity components $\Delta\mathbf{u}_{\mathrm{rad}}$ (red) and $\Delta\mathbf{v}_{\mathrm{rot}}$ (blue) of the galaxy groups and clusters at different distances (near: yellow; far: pink) are shown relative to the motion of the Local Group (green). **c**, Simulated contour map of the Hubble constant.

where C_{rot} is the proportional constant for the velocity component of rotation. For the simulation of the Hubble constant in the local universe ($z = 0.1$), we assume the minimum number of parameters: $H_{0,\,\mathrm{iso}} = 67.4$ km s^{-1}Mpc^{-1} , $\mathbf{v}_{\mathrm{rad}} = 53{,}000$ km s^{-1} , $\mathbf{v}_{\mathrm{rot}} = 38{,}000$ km s^{-1} (equivalent to an angular velocity $\omega = 1.5 \times 10^{-19}$ s^{-1}, which is about one order of magnitude less than that from the Gödel metric[36,37]), and $C_{\mathrm{rot}} = 1.25$ km s^{-1}Mpc^{-1} (equivalent to a speed of 500 km/s at 400 Mpc, which is less than C_{BF} and hence reasonable). The simulated map is shown in Fig. 8c, impressively close to Migkas *et al.*'s observations in the local universe (fig. 21 in ref.[51]). Some key results are: the lowest $H_0 = 66.3$ km s^{-1}Mpc^{-1} at $(l, b) = (267°, -26°)$; and the highest $H_0 = 75.6$ km s^{-1}Mpc^{-1} at $(l, b) = (6°, -12°)$. For comparison, Migkas *et al.*'s results[51] are: the lowest $H_0 = 66.20 \pm 1.72$ km s^{-1}Mpc^{-1} at $(l, b) = (274°, -22°)$; and the highest $H_0 = 75.17 \pm 1.81$ km s^{-1}Mpc^{-1} at $(l, b) = (17°, -9°)$. It is important to note that as long as the center and the rotation are applied to the simulation, similar patterns of the anisotropy can always be obtained even if the parameters are assumed differently in reasonable ranges (meaning that the best results may not have been obtained yet), which strongly supports our finding.

Another interesting point would be the constants that we assumed for the simulation. The Hubble constant representing the isotropic expansion, $H_{0,\,\mathrm{iso}} = 67.4$ km s^{-1}Mpc^{-1}, is the same as that from the CMB[12]. If we calculate it at the Local Group, $H_0 = \left(67.4 + \frac{53{,}000}{9.3 \times 10^3}\right)$ km s^{-1}Mpc^{-1} = 73.1 km s^{-1}Mpc^{-1}, which is the same as what Riess *et al.* observed in the local universe[52]. We therefore wonder if the Hubble tension[52,53] could be related to the anisotropic expansion of the universe[54]. For the infant universe when it emitted the CMB, though it spun much faster, the contribution on the Hubble constant from the spinning (as well as the vacuum energy) was insignificant. Other observations such as the sigma-8 tension[55] would be due to the same reason.

The fourth evidence is about the nucleation centers from the precursor. The emission beams V_b, the back falling flows V_f, and the falling spiral flows V_s around the core of the precursor black hole, a hypoatom star or neutrino star, would act as nucleation centers or seeds for the formation of the astronomical objects in our universe.

As discussed above, the falling spiral flows V_s were not continuous (Fig. 5). The precursor core before the Big Bang was so small in diameter (only ca. 2 m), so the emission beams V_b and the back falling flows V_f (Fig. 5) would sweep in a high angular speed, producing discontinuous clumps of high-density energy and/or matter across the space within the event horizon of the precursor black hole. During the early expansion of the Big Bang, these flows would collide with the powerful radial expansion waves V_{BB} of the Big Bang, resulting in more clumps and debris as nucleation centers for the new universe. Compared to the ΛCDM model in which nucleation centers were generated by quantum fluctuations, our model provides a mechanism to have nucleation centers much earlier, and hence explains multiple extraordinary astronomical facts.

As the universe cools down, the clumps of high-density energy and/or matter would collapse into primordial supermassive black holes, while attracting surrounding matter to form the first galaxies. Small debris would also form directly into the first stars while being attracted by nearby galaxies.

Primordial supermassive black holes and the first galaxies would be formed anywhere across the sky, because the clumps of high-density energy and/or matter would be sprayed anywhere within the event horizon (Figs. 5 and 9). However, the distribution

would not be isotropic or homogeneous; some sky zones would have higher densities. The first would be Zone C, surrounding the center of the universe (Fig. 9). As all the flows were either falling into or emitting to the core, a high density of the nucleation centers would be produced nearby. Therefore, a high density of supermassive black holes and the first galaxies would be observed in the direction of the center of the universe. The equator plane would have higher densities, though a large part of it would be in the Zone of Avoidance. Zone N in the North half-ball and Zone S in the South half-ball, which have a latitude viewing from the center, i.e. the angle with the equator, lower than 58° (Fig. 9), would be two large high-density zones, if the emission beams V_b is assumed to fall into the equator plane more directly (Fig. 5).
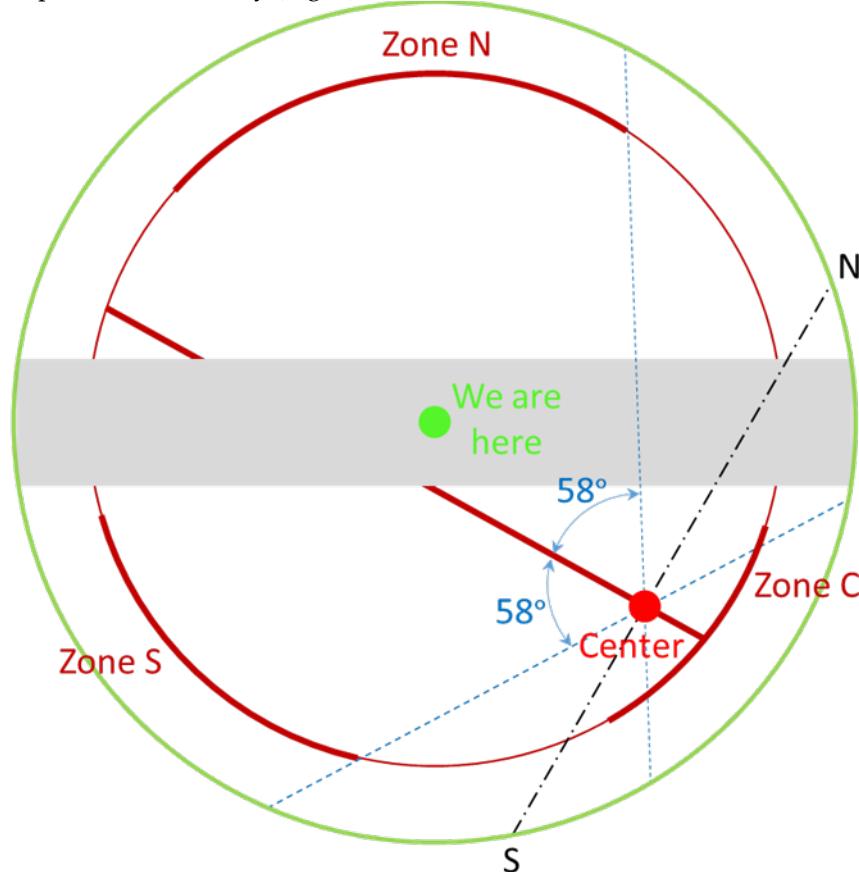
Fig. 9. Anisotropic distribution of the first galaxies. The first galaxies would be found more frequently in the following high-density zones. Zone C (dark red arc) is near the center of the universe (red dot). The intersected zone between the equator plane (dark red line) and the spherical surface (dark red circle) of a radius of 11.5 Gpc (z~30) where the universe was 100 million years after the Big Bang. Zone N (dark red arc) is located in the North half-ball, with the latitude viewing from the center (red), i.e. the angle with the equator (dark red line), lower than 58°. Zone S is located in the South half-ball, with the latitude lower than 58°. The center dot (green) represents where we are or the LG, and the largest circle (green) is the SLS. The horizontal wide zone (grey) represents the Zone of Avoidance. This schematic diagram is not in accurate scale.

Of all these zones, Zone C would have the highest number and mass density of the first galaxies. However, because the collisions near the center are the strongest, the debris or seeds would be formed with relatively smaller masses. Therefore, individuals of black holes and the first galaxies would not have masses as high as those formed in other zones.

Note that the energy density of the universe was distributed almost uniformly because the V_{BB} was dominating. Compared to that from the Big Bang, the energy or mass that the nucleation centers carried from the precursor black hole would be negligible. Even

the distribution of the seeds was not homogeneous in the infant universe. As the universe grows, an almost homogeneous distribution of the galaxies has been observed.

The James Webb Space Telescope (JWST) has shown its power to observe the first galaxies. The primary results indicate that there are lots of distant, complex galaxies[56,57]. These results perfectly match our model. With the existence of the nucleation centers or seeds from the precursor black hole, the formation process of the first galaxies would be much faster than predicted by the ΛCDM model or the cosmological principle. We believe that the first galaxies would be formed even earlier than 250 million years after the Big Bang. Fig. 9 was prepared at a radius where the universe was 100 million years after the Big Bang. The seeds would also speed up the growth of the galaxies and develop more complex galaxies, such as disk-shaped galaxies. The large number of debris from the collisions of the flows would result in so many distant galaxies observed by the JWST.

Other than black holes and galaxies, the nucleation centers would also generate other large cosmic structures or objects. One category is extraordinarily large great walls, particularly those whose sizes are incompatible with the cosmological principle, such as the Hercules–Corona Borealis Great Wall, Giant GRB Ring, and Huge-LQG, etc. Another category is extraordinarily supermassive black holes, particularly those whose masses exceed the theoretical limits, such as Phoenix A, TON 618, and MS 0735.6+7421, etc.

3.5. Fate of the universe

Based on our model, the universe is a flat, open system; the fate of the universe would end up with many new Big Bangs. This naturally explains the accelerating expansion of the current universe. Black holes, or their mergers, would be the seeds of the universes of the next generation, and hence require space or energy to grow. Our universe is still at her young age!

Acknowledgements

J.B.B. would like to thank Profs. Z. Shen, K. Yao, X. Jiang, F. Bo, Y. Cheng, S. Han, G. Chen, and Q. Yu at Zhejiang University for their inspiration. N.P.B. would like to dedicate this work to his grandparents in China.

References

1. Einstein, A. Ether and the theory of relativity (Address Univ. Leiden, 5 May 1920).

2. Guth, A. H. Inflationary universe: a possible solution to the horizon and flatness problems. *Phys. Rev. D* **23**, 347-356 (1981).

3. Linde, A. D. A new inflationary universe scenario: a possible solution of the horizon, flatness, homogeneity, isotropy and primordial monopole problems. *Phys. Lett.* **108B**, 389-393 (1982).

4. Kolb, E. W. & Turner, M. S. The early universe (Addison-Wesley, Redwood, 1990).

5. Starobinsky, A. A. Multicomponent de Sitter (inflationary) stages and the generation of perturbations. *JETP Lett.* **42**, 152-155 (1985).

6. Silk, J. & Turner, M. S. Double inflation. *Phys. Rev. D* **35**, 419-428 (1987).

7. Sinha, K. P., Sivaram, C. & Sudarshan, E. C. G. Aether as a superfluid state of particle-antiparticle pairs. *Found. Phys.* **6**, 65-70 (1976).

8. Pethick, C. J. & Smith, H. Bose-Einstein condensation in dilute gases (Cambridge Univ. Press, Cambridge, 2002).

9. Schive, H.-Y., Chiueh, T. & Broadhurst, T. Cosmic structure as the quantum interference of a coherent dark wave. *Nat. Phys.* **10**, 496-499 (2014).

10. Dirac, P. A. M. Is there an aether? *Nature* **168**, 906-907 (1951).

11. Fagnocchi S. *et al*. Relativistic Bose-Einstein condensates: a new system for analogue models of gravity. *New J. Phys.* **12**, 095012 (2010).

12. Planck Collaboration: Aghanim N. *et al*. Planck 2018 results. VI. cosmological parameters. *Astron. Astrophys.* **641**, A6 (2020).

13. Linde, A. D. The inflationary universe. *Rep. Prog. Phys.* **47**, 925-986 (1984).

14. Guth, A. H. Lecture 23: inflation (MIT Open Course Ware, 2013).

15. Weiler, T. Resonant absorption of cosmic-ray neutrinos by the relic-neutrino background. *Phys. Rev. Lett.* **49**, 234-237 (1982).

16. Weiler, T. J. Cosmic-ray neutrino annihilation on relic neutrinos revisited: a mechanism for generating air showers above the Greisen–Zatsepin–Kuzmin cutoff. *Astropart. Phys.* **11**, 303-316 (1999).

17. Formaggio, J. A. & Zeller, G. P. From eV to EeV: neutrino cross sections across energy scales. *Rev. Mod. Phys.* **84**, 1307-1341 (2012).

18. IceCube Collab., Measurement of the multi-TeV neutrino interaction cross-section with IceCube using Earth absorption. *Nature*, **551**, 596-600 (2017).

19. Barbieri R. *et al*., Baryogenesis through leptogenesis. *Nucl. Phys. B* **575**, 61-77 (2000).

20. Abada A. *et al*., Flavour matters in leptogenesis. *J. High Eng. Phys.* **09**, 010 (2006).

21. Grossman, Y. & Tanedo, P. Chapter 4: just a taste: lectures on flavor physics. Anticipating the Next Discoveries in Particle Physics. pp. 109-295 (World Scientific, Singapore, 2018).

22. Olive, K. A. *et al*. (Particle Data Group), Review of particle physics. *Chin. Phys. C* **38**, 090001 (2014).

23. Agostini, M. *et al*. (Borexino Collaboration), Test of electric charge conservation with Borexino. *Phys. Rev. Lett.* **115**, 231802 (2015).

24. https://en.wikipedia.org/wiki/Proton_decay.

25. Taylor, E. F., Wheeler, J. A. & Bertschinger, E. Exploring black holes: introduction to general relativity. 2nd ed. (Addison-Wesley, Redwood, 2010).

26. Moore, B. *et al*. Resolving the structure of cold dark matter halos. *Astrophys. J.* **499**, L5-L8 (1998).

27. Feynman, R. P., Leighton, R. B. & Sands, M. The Feynman lectures on physics: quantum mechanics. The new millennium ed. vol. III (Basic books, New York, 2010).

28. Van der Klis, M. *et al*. Intensity-dependent quasi-periodic oscillations in the X-ray flux of GX 5-1. *Nature* **316**, 225-230 (1985).

29. https://images.nasa.gov/details-PIA21418.

30. Prakash, N. Dark matter, neutrinos, and our solar system (World Sci., Singapore, 2013).

31. Perkins, D. Particle Astrophysics. 2nd ed. (Oxford Univ. Press, New York, 2003).

32. http://pla.esac.esa.int/pla/#maps.

33. Cruz, M. *et al*. A cosmic microwave background feature consistent with a cosmic texture. *Science* **318**, 1612-1614 (2007).

34. Gott III, J. R. *et al*. A map of the universe. *Astrophys. J.* **624**, 463-484 (2005).

35. Kovács A. *et al*. The DES view of the Eridanus supervoid and the CMB Cold Spot. *MNRAS*, **510**, 216-229 (2021).

36. Gödel, K. An example of a new type of cosmological solutions of Einstein's field equations of gravitation. *Rev. Mod. Phys.* **21**, 447-450 (1949).

37. https://en.wikipedia.org/wiki/Gödel_metric.

38. Hawking, S. On the rotation of the universe. *MNRAS* **142**, 129-141 (1969).

39. https://en.wikipedia.org/wiki/Big_Bang.

40. https://en.wikipedia.org/wiki/Lemaître-Tolman_metric.

41. Gamow, G. Rotating universe? *Nature* **158**, 549 (1946).

42. Longo, M. J. Detection of a dipole in the handedness of spiral galaxies with redshifts z ∼ 0.04. *Phys. Lett. B* **699**, 224-229 (2011).

43. Shamir, L. Handedness asymmetry of spiral galaxies with z < 0.3 shows cosmic parity violation and a dipole axis. *Phys. Lett. B* **715**, 25-29 (2012).

44. Hutsemékers D. *et al*. Mapping extreme-scale alignments of quasar polarization vectors. *Astro. Astrophys.* **441**, 915-930 (2005).

45. Hudson M. J. *et al*. A large-scale bulk flow of galaxy clusters. *Astrophys. J.* **512**, L79-L82 (1999).

46. Kashlinsky A. *et al*. A measurement of large-scale peculiar velocities of clusters of galaxies: results and cosmological implications. *Astrophys. J.* **686**, L49-L52 (2008).

47. Migkas K. *et al*. Cosmological implications of the anisotropy of ten galaxy cluster scaling relations. *Astro. Astrophys.* **649**, A151 (2021).

48. Nusser, A. & Davis, M. The cosmological bulk flow: consistency with ΛCDM and z ≈ 0 constraints on σ_8 and γ. *Astrophys. J.* **736**, 93 (2011).

49. Salehi, A., Yarahmadi, M. & Fathi, S. The cosmological bulk flow in QCDM model: (in)consistency with ΛCDM. *MNRAS* **504**, 1304-1319 (2021).

50. Planck Collaboration: Ade, P. A. R. *et al*. Planck intermediate results. XIII. constraints on peculiar velocities. *Astron. Astrophys.* **561**, A97 (2014).

51. Migkas K. *et al*. Probing cosmic isotropy with a new X-ray galaxy cluster sample through the L_X-T scaling relation. *Astro. Astrophys.* **636**, A15 (2020).

52. Riess, A. G. *et al*. A comprehensive measurement of the local value of the Hubble constant with 1 km/s/Mpc uncertainty from the Hubble Space Telescope and the SH0ES team. arXiv:2112.04510v2, 2022.

53. Riess A. G. *et al*. Large Magellanic Cloud Cepheid standards provide a 1% foundation for the determination of the Hubble constant and stronger evidence for physics beyond ΛCDM. *Astrophys. J.* **876**, 85 (2019).

54. Colin J. *et al*. Evidence for anisotropy of cosmic acceleration. *Astron. Astrophys.* **631**, L13 (2019).

55. Battye, R. A., Charnock, T. & Moss, A. Tension between the power spectrum of density perturbations measured on large and small scales. *Phys. Rev. D* **91**, 103508 (2015).

56. Witze, A. Four revelations from the Webb telescope about distant galaxies. *Nature* **608**, 18-19 (2022).

57. Clery, D. Webb reveals early universe's galactic bounty. *Science* **377**, 700-701 (2022).